Journal of Electronics and Electrical Engineering
https://ojs.wiserpub.com/index.php/JEEE

Optimization and Impact Analysis of PV Penetration in Radial Distribution System: A Case Study of Panbari Feeder

Hari Bhusal[1*], Amrit Parajuli[1], Srijan Khadka[2], Radhika Kumari Sah[3] and Shailendra Kumar Jha[1,4]

[1] Department of Electrical and Electronics Engineering, Kathmandu University, Dhulikhel, Kavre, 6250, Nepal
[2] Department of Electrical Engineering, Khwopa College of Engineering, Libali, Bhaktapur, 44800, Nepal
[3] Department of Electrical Engineering, National College of Engineering, Talchhikhel, Lalitpur, 44700, Nepal
[4] Department of Electric Energy, Norwegian University of Science and Technology, Torgarden, Trondheim, Norway
*E-mail: hari.bhusal@ku.edu.np

Received: 2 April 2025; **Revised:** 19 June 2025; **Accepted:** 24 June 2025

Abstract: The integration of distributed generation is one of the most effective alternative methods for enhancing the voltage profile and reducing power loss in radial distribution systems. This study investigates the impact of integrating photovoltaic (PV) generation on distribution systems, considering radial distribution networks. The IEEE 33 bus radial distribution system and Panbari feeder of the Dharan substation are selected as candidate systems. Particle Swarm Optimization (PSO) and Genetic Algorithm (GA) are proposed for determining the optimal location and sizing of single and multiple PV installations, considering minimum power loss as the objective function. The results are analyzed in terms of voltage profile improvement and power loss minimization with PV integration. Additionally, a comparative analysis is conducted for the system with PV integration and PV with capacitor bank for reactive power injection. An economic analysis is performed to determine the optimal number of Distributed Generator (DG) integrations. Through sensitivity analysis, the most sensitive buses are identified, and Power-Voltage (P-V) curves are plotted for these buses in the base case and cases after integration of PV only and PV with capacitor banks. The results are examined and compared in terms of load margin limit and critical voltage point. Among single and multiple PV integrations, the integration of two PV installations is found to be most suitable based on economic analysis. Simulation results demonstrate that the integration of PV sources in existing radial distribution systems has a positive impact on steady-state voltage stability. Furthermore, improvements in voltage profile and significant reductions in system power loss are observed.

Keywords: PV integration, Voltage stability, Radial Distribution System, Panbari feeder, Metaheuristic optimization

1. Introduction

The use of Renewable Energy Sources (RES) has increased significantly over time in recent years. Sources such as PV and wind energy are used to generate electricity for various purposes. It involves integrating different renewable energy sources (RES) with existing power grids to provide consumers with reliable and high-quality electricity. Being widely used on a global scale, solar power generation is a significant component of Renewable Energy Sources (RES) [1]. The integration of PV can be observed on a large scale, where high power is directly injected into power grids, and on a small scale, for distribution networks using PV as an individual distributed generator (DG) [2], [3]. Distributed Generation is the integration of an electrical power generation system in the consumer end of the distribution network. The individual unit on the consumer end is the Distributed Generator [4]. The abundance of research and development in advanced PV technology makes it one of the most effective

DOI: 10.37256/jeee.4220256908

systems for working as a distributed generation source, which is integrated into many real-world systems [5]. When integrating PV systems into the grid, it's essential to consider that their power output can fluctuate, as solar energy is an intermittent source. As a result, modeling solar PV is crucial to capture its variable nature[6].

Most conventional distribution networks are designed radially, with a centralized generation source supplying power to the entire linear grid in a single direction.[7]. In this distribution network, when power on the demand side increases, the system needs to supply more power which in turn increases the power loss and decreases the voltage stability of the system[8]. At this point, the system becomes less efficient and more costly as loss increases, and reliability decreases. To overcome this situation, DG with RES is introduced in the system. DG makes the system able to use reverse power flow, i.e., power flow from DG at the consumer end to the primary generating source[9]. Among the only few sustainable alternative sources of energy, the PV system can be used as the best DG source[10]. Social acceptance of PV systems mainly is of localized concerns, like land-use conflicts and community benefits [11]. Systems with aesthetically integrated PV designs can improve people's adoption by addressing visual and spatial preferences [12], [13].

The idea of integrating PV in the distribution system may be promising, but it is not an outright solution. It directly does not solve the problems of a system. PV penetration may exhibit both positive and negative impacts on an existing system. It depends on various factors, such as size and location.

2. Related Works

Key issues, such as voltage fluctuations, elevated voltage levels, phase voltage imbalances, and the introduction of harmonics, influence grid stability and performance, and these can be observed due to PV penetration [14]. At the lower level of PV integration, PV inverters do not have a significant impact, but at higher penetration levels, PV inverters may be sufficient to provide all the feeder voltage support [15]. [16] highlights that a voltage rise on the feeder is a common effect wherever PV systems are installed. The impact of solar photovoltaic generation on power network static voltage stability can be studied using PV curves [17]. [18] assesses the maximum PV integration in Hebron's sub-grid during summer, by modeling grid constraints like line congestion, substation overload, and voltage rise at varying PV penetration levels. Results demonstrate that the grid can support 37.53 MW of low-voltage (LV) and 21.89 MW of medium-voltage (MV) PV without exceeding operational limits, including transformer capacity, cable ampacity, and voltage stability, indicating substantial potential for solar deployment while maintaining reliability. In [19] the effect of PV penetration is investigated in the distribution system showing that the low level of PV integration improves the system voltage profile and minimizes the overall power losses in the system by reducing the total power demand from the substation, but as the integration of the PV exceeds the integration limits, the voltage range set by ANSI gets violated and the system losses start increasing. [20] investigates the influence of Self-Consumption Rate (SCR) on voltage quality in low-voltage (LV) radial networks. Analyzing the standard IEEE LV feeder model and random load profiles, various simulations are conducted to determine the relationship between prosumers' SCR and voltage performance. The results indicate that beyond a certain SCR threshold, overvoltage issues do not occur in the LV feeder. [21]presents a novel methodology for designing and analyzing hybrid wind-photovoltaic off-grid systems with battery storage, demonstrating their technical and environmental feasibility for powering small remote settlements. [22] examines the impact of integrating photovoltaics (PV) into distribution networks, primarily its effects on harmonic distortion levels. Key aspects, such as the DG penetration level, the number of DG units, and their distribution, are analyzed to study the harmonic behavior within the system. Noting that the most effective output, optimum placement, and optimal penetration level are key factors, it concludes that analysis is necessary to determine the optimal size and location before connecting PV to the existing radial distribution feeder. As the integration of DG into distribution grids is increasingly addressed with hybrid systems, life cycle assessment (LCA), and multi-criteria planning frameworks are considered for balancing technical, economic, and environmental factors [23]. Hybrid systems, such as PV-wind-battery configurations, improve grid stability and resource utilization, as evidenced by optimized hybrid power plants with dynamic transformer ratings [24]. The hybrid LCA approach helps understand the impacts analysis of PV integration in distribution systems by incorporating full life-cycle environmental impacts, such as embodied energy and emissions [25]. Together, these methods support holistic planning, which ensures PV integration aligns with grid reliability, ecological goals, and socio-economic priorities [26], [27].

Several research studies for impact assessment and optimization of PV size and placement have been performed to find and overcome these problems (issues), i.e., power loss reduction and improvement of voltage profile. Among the various heuristic approaches used for DG placement studies in radial distribution systems, GA and PSO are both population-based stochastic optimization methods [28]. The PSO reaches the same optimum solution if the size range is chosen as high as close to the total load demand [29]. An optimal location for a solar

generator with a connected Energy Storage System (ESS) is required before installation, as it is not possible to adjust the location of power injection into the system due to changes in loads or cases of congestion [30]. [31] proposes the optimal placement and sizing of PV systems with batteries and diesel hybrid systems to reduce the overall system cost and control grid voltage using PSO. In [32], the most sensitive bus in the network (IEEE-39 bus test distribution system) is selected for DG placement. By finding the optimal number of DG placements, computing system power losses (increasing the value of DGs' number in each iteration and computing load flow), this method is seen as efficient in improving voltage profile, reducing losses, and increasing line loading capacity. Here, the L index (Voltage Collapse Index), VPI (Voltage Profile Improvement) index, and LSF (Loss Sensitivity Factor) index are used for the sensitivity analysis of the individual buses. The L-index, VPIs, and LSFs have been evaluated for every load bus, and the best DGs' locations have been identified based on higher values of L-index and VPI, unlike LSF, where lower values refer to optimal locations.[28] demonstrates the probabilistic model taking account of solar irradiance in the Radial Distribution System (RDS). For the model, load and DG production are treated as random variables, and the proposed JFPSO is shown to have minimal standard deviation and high accuracy in comparison with the standard BPSO and GA for DG location and size optimization. [29] shows the multi-objective function (including active power loss, reactive power loss, MVA capacity index, and voltage profile index) used in PSO for DG size and location optimization. The proposed PSO algorithm tested was found to be more efficient, showing a greater reduction in power loss with a smaller DG size in the IEEE 33 RDS. [31] shows that PSO is used for optimizing the size and location of DG, considering cases of PV only and PV with an energy storage system. Results showed that during a day, the voltage profile of the DG + PV + battery system can keep the voltage within tolerable limits. The research [33] demonstrates the optimization of hybrid energy systems combining PV, wind, and biomass using PSO and GA. The minimization of energy costs is used as the objective function for the optimization problem. In optimizing battery charging strategies for hybrid energy storage, PSO outperforms GA. [34] shows PSO used for DG placement and sizing optimization using the minimization of active power loss as the objective function. The results showed a reduction in power line losses and an improved voltage profile. In [35], the author implemented a Decision-making algorithm that is highly flexible to changes and modifications and can define the optimal size and location for a DG. This approach is proposed and has been tested in the IEEE 33 RDS. Not considering parameters such as annual load variability and economic factors associated with DG installation, the proposed algorithm appears to be efficient and can provide reasonable solutions for determining the optimum size and placement of DG units in distribution networks [36]. [37] used CLPSO for optimal sizing and placement of DG in the IEEE 33 bus and compared the result with the standard PSO algorithm. The findings revealed that CLPSO outperforms standard PSO in maximizing loss reduction. [38] demonstrates a hybrid approach (a combination of analytical methods and heuristic search) being adopted for DG sizing and placement, and the result is validated by comparing the results obtained using PSO. Testing on the IEEE 33 bus system, the hybrid approach has shown slightly better results than PSO in terms of loss reduction—a Novel hybrid PSO (HPSO) with a Quasi-Newton (QN) algorithm proposed for DG placement. The loss sensitivity analysis is employed to determine the optimal DG location, and then HPSO is used to find the size of the DG at this location. Compared to GA, PSO, GA/PSO, SA, and BFOA, the proposed algorithm shows a high accuracy and performance solution [39]. [34] Introduces sensitivity analysis to determine the optimal sitting and sizing of DG units.

Integration of PV systems in the electric power grid itself is a challenging task due to the stochastic nature of PV generation [40]. Unsupervised integration of PVs in electric power systems can lead to different issues such as changes in power quality, power flow imbalance between generation and load demand, and voltage and frequency variation [41], [42]. Due to the intermittent nature of the PV system, various problems may arise under varying load demands. It can have a critical impact on the performance of the power system. While load demand is less and the power output of the PV system is greater, there may arise the problem of overvoltage in the distribution system. If load demand is high and the production of the PV is less, then (despite adding the DG), there will be no positive impact, and under-voltage will prevail on the system [43]. Likewise, if DG placement is random and not optimized, problems of increased power loss and over-voltage in the nearest buses are seen. When DG is placed very far from the load side, power loss increases rather than decreases (for which the DG was placed), and the voltage profile is not improved. If the DG is placed near the load side, the power loss will decrease, and the system's voltage level will be maintained. The placement position and size of the PV penetration can affect the working of the distribution system [44]. Therefore, optimizing PV placement and size is necessary to minimize losses and improve the voltage profile within the desired limits of the distribution system.

To summarize, the severity of the issues associated with PV or other types of distributed generation (DG) integration depends on the level of penetration, the distribution system's structure, and the placement of PV units within the distribution system. In such cases, a high-level PV penetration can inject power into the transmission network, potentially affecting the voltage level and protection settings of the distribution system. In contrast, low-

level penetration may not yield the desired outcome of a decrease in active power loss and improvement in voltage profile. Under these conditions, the distribution system operates as an active network. Therefore, the study of the impact of distributed generation (DG) integration on the distribution system is crucial. In this regard, the primary contributions of this research are highlighted as follows:

- The study proposes a methodology that identifies the optimal penetration level and placement of PV in the existing distribution system, noting the impacts of integration.
- An economic analysis is conducted to determine the most suitable number of DG integrations, and its impact on steady-state voltage stability is observed.

The remaining portion of the article is structured as follows: Section 3 describes the algorithm used to optimize the PV location and size, as well as the economic analysis and voltage stability analysis. Section 4 focuses on the study of the obtained results for the IEEE 33 bus radial distribution system (RDS) and Panbari feeder. Finally, Section 5 presents the findings of the research and concludes the article.

3. Methodology

The block diagram of the complete methodology is shown in Figure 1. The proposed methodology has four steps: Step 1: Initialization, Step 2: Optimization of PV placement and size, Step 3: Technical and Economic Analysis, and Step 4: Voltage Stability Analysis, which are described in detail in the following subsections.

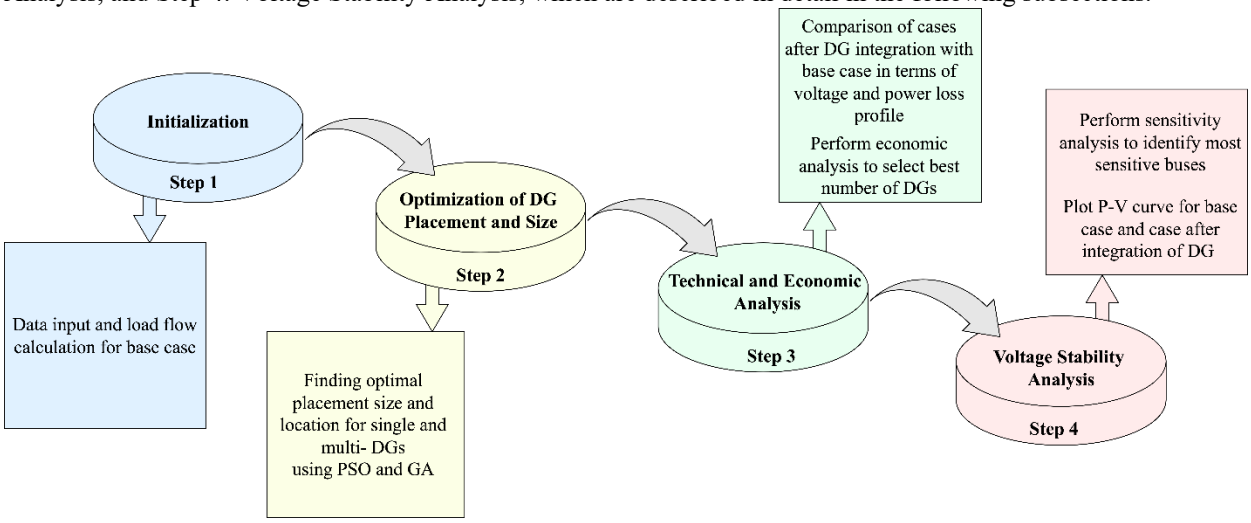

Figure 1 Methodology of the proposed research

3.1. Initialization

Characteristics of distribution systems, such as the high resistance-to-reactance (R/X) ratio and the radial structure with numerous nodes and branches, the integration of DG units, and complex configurations, make it unfavorable to be addressed with a conventional iterative approach [45]. So, for this study, the load flow is done using the Backward Forward Sweep Algorithm.

3.1.1. Backward Forward Sweep Algorithm

The complete flow diagram of the Backward Forward Sweep Algorithm is shown in Figure 2. It begins by initially setting the voltage value to 1 p.u. at all nodes. Then, during backward sweep propagation, the node current is calculated using (1), and the current flowing from the ith node to the (i+1) th node is determined using (2). After computing the branch current, the voltage at the ith node is calculated using (3). This step continues till the junction node is reached. At the junction node, the voltage computed is stored.

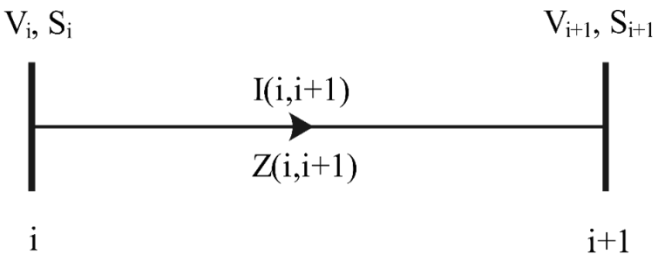

Figure 2 Single Line Diagram with Two Nodes

In Figure 2, Vi is the voltage at ith node, Si is the apparent power at ith node, Vi+1 is the voltage at (i+1)th node, Si+1 is the apparent power at (i+1)th node, I(i,i+1) is the current flowing from ith node to (i+1)th node and Z(i,i+1) is the impedance of the line.

$$I_i = (S_i/V_i)^* \tag{1}$$

$$I(i,i+1) = I_{i+1} + \sum currents\ in\ branches\ emanating\ from\ node(i+1) \tag{2}$$

$$V_i = V_{i+1} + I(i,i+1) * Z(i,i+1) \tag{3}$$

Now, starting with another end node of the system, voltage, and current are again calculated. The current at the junction node is calculated using the most recent voltage at the junction node using (1). Compute the current and voltage till the reference node is reached. When the reference node is reached, compare the calculated magnitude of the rated voltage at the reference node with the specified source voltage. If the voltage difference is less or equal to the Tolerable Limit (Tlimit) (for this case, Tlimit = 10-6 V), then the process is stopped and the value of current and voltage is stored, otherwise, forward sweep propagation is started. In forward sweep propagation, starting with the reference node at rated voltage, the node voltage in the forward direction from the reference node to the end nodes is calculated using (4). Again, the backward sweep starts with the updated bus voltage calculated in the forward sweep.

$$V(i+1) = V_i - I(i,i+1) * Z(i,i+1) \tag{4}$$

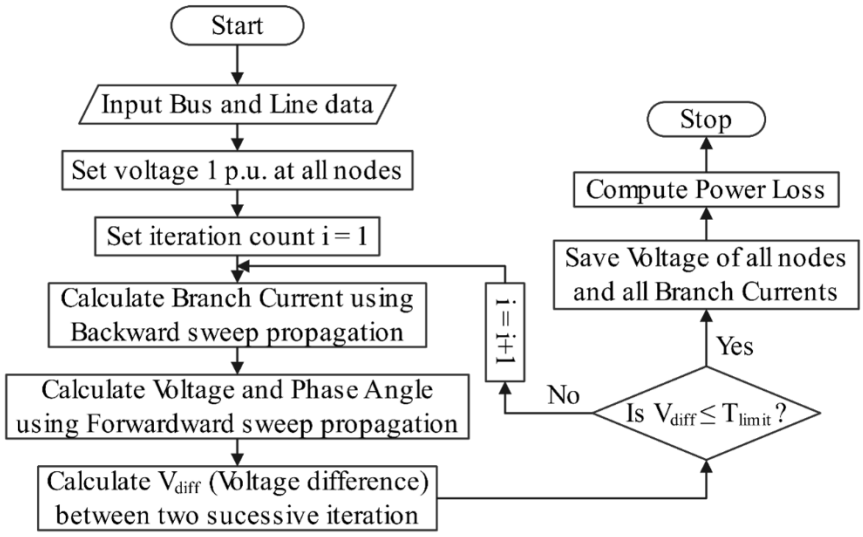

Figure 3 Flowchart for Backward Forward Sweep Algorithm

After calculating node voltages and line currents using the standard BW/FW sweep algorithm, the line losses are calculated. The complex power, Si,i+1 from the ith bus to (i+1)th bus and Si+1, i from (i+1)th bus to ith bus, are calculated using (5) and (6). The voltage and power at ith and (i+1)th node are shown in Figure 3.

$$S_{i,i+1} = (V_i * I_{i,i+1})^* \tag{5}$$

$$S_{i+1,i} = (V_{i+1} * I_{i,i+1})^* \tag{6}$$

The voltage, active, and reactive power loss at each bus for the radial distribution network are calculated using (1) - (6) for the base case. After computing the voltage, current, active, and reactive power losses, the values are stored and used during optimization.

3.1.2. Mathematical formulation of the optimization problem

The primary objective of the proposed methodology is to minimize real power loss while subject to various constraints. This can be mathematically expressed as:

$$F(x) = \min \sum_{i=1}^{N} P_{i\,loss} \tag{7}$$

Where, F(x) is Objective Function and $i \in [1,2,3, \dots, N]$, $N \in 1,2,3$.

The objective function is subject to several constraints, including branch capacity limit, voltage magnitude limit, PV power rating, active and reactive power loss, and the location for PV placement, which need to be considered before starting the optimization. The branch capacity limit of the distribution system can be represented by the current flowing between two nodes (buses) i and j, which can be expressed as:

$$I_{(i,j)} \leq I_{rated} \tag{8}$$

The voltage magnitude must be within the required limit, ensuring no problems with under-voltage and over-voltage in the system. For our case, it is taken between 0.95 p.u. and 1.05 p.u. i.e.,

$$0.95 \leq |V_i| \leq 1.05 \tag{9}$$

The algorithm is designed such that the active and reactive power losses after PV integration must be less than the active and reactive power losses before PV integration. It can be expressed as:

$$P_L \text{ with PV} \leq P_L \text{ without PV} \tag{10}$$

$$Q_L \text{with PV} \leq Q_L \text{without PV} \tag{11}$$

The level of PV penetration also has crucial impacts on the radial distribution system. It must be such that it has some positive impacts, i.e., improving the voltage level in the system and reducing power loss compared to the base cases. Its level of penetration must not exceed the total load connected to the system. It can be given as;

$$0 \leq \sum_{i=1}^{N} P_{PV,i} \leq \sum_{i=1}^{N} P_{L,i} \tag{12}$$

Where, $i \in [1,2,3, \dots, N]$, PPV is the level of PV penetration, and PL is the total load connected to the system.

The location of PV should be optimal and must be inside the distribution system. In our case, the location should be a node for a single PV system. If 'N' is the number of PV systems, then there should be 'NL' locations.

Where, $N \in 1,2,3$.

For,

N=1, NL= 1 locations

N=2, NL= 2 locations

N=2, NL= 3 locations.

3.2. Optimization of PV placement and Size

Optimization is to be performed for PV sizing and location to determine optimal penetration after storing the base case data and formulating the problem in the distribution system. For the optimal location of single and multi-PV penetration, two evolutionary optimization algorithms —Particle Swarm Optimization (PSO) and Genetic Algorithm (GA) — were used and are described in detail in subsections 3.2.1 and 3.2.2. To minimize the power loss as the objective function, optimization was carried out for two distinct scenarios: (a) PV-only Integration and (b) PV with Capacitor Integration. For both scenarios, $N \in [1, 2, 3]$.

3.2.1. Particle Swarm Optimization

The detailed workflow of the PSO algorithm is shown in Figure 4. The process begins by initializing a random population, where the objective function, defined in equation (7), is evaluated for each swarm particle in the population. Each particle records its best solution in the hyperspace, termed the personal best (Pbest), which corresponds to the optimal solution it has achieved individually. Additionally, the algorithm maintains the global best (Gbest) value, which is the highest fitness value among all swarm particles in the population. During each iteration, the PSO changes the velocity of every particle, guiding its movement toward both its Pbest and the Gbest positions and updating the location in the search space. This iterative process continues until a predetermined number of iterations is completed, at which point the optimized solution is found. The velocity and position of the ith particle are given by equations (13) and (14) [46]

$$V_{in}^{(t+1)} = w * v_{in}^{(t)} + c_1 * rand * \left(p_{best\,in} - x_{in}\right) + c_2 * rand * \left(g_{best_{in}} - x_{in}\right) \quad (13)$$

$$X_{in}^{(t+1)} = x_{in}^{(t)} + v_{in}(t+1) \quad (14)$$

When the number of iterations is completed, the optimized results are presented. For the proposed methodology, the values of the parameters used in the optimization algorithm are mentioned in Appendix A.11.

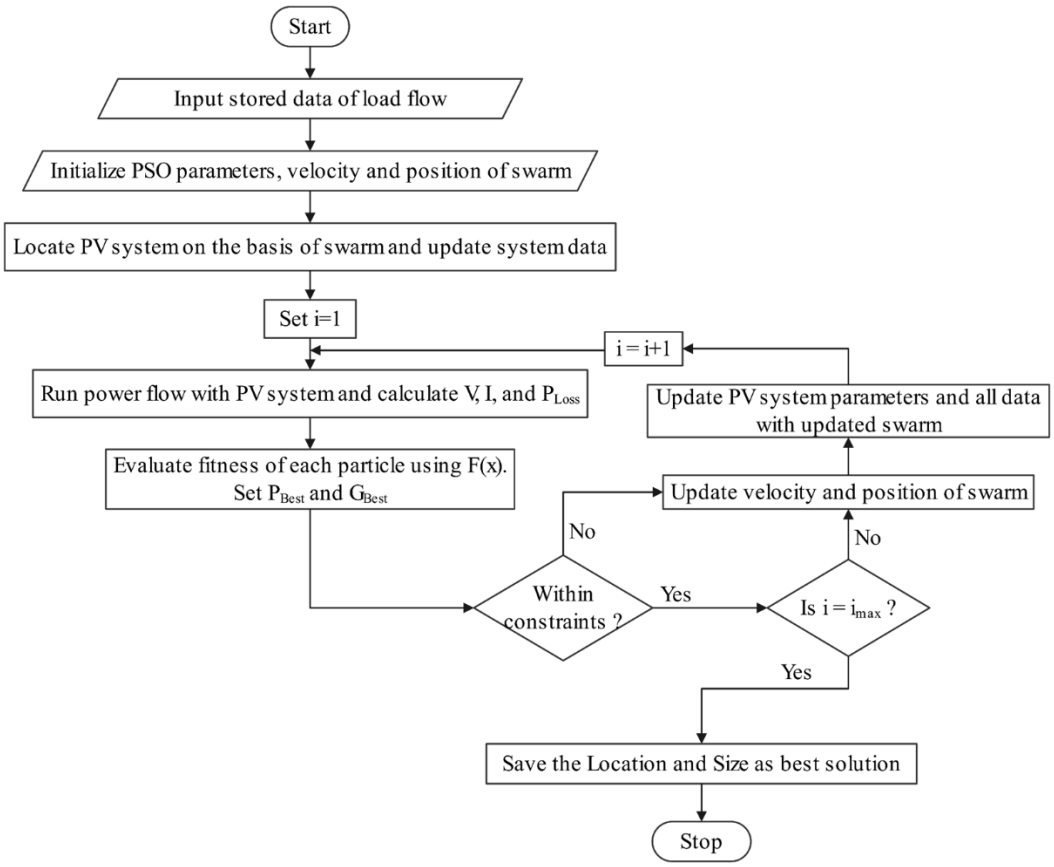

Figure 4 Flowchart for Optimal Placement and Size of PV system using PSO

3.2.2. Genetic Algorithm (GA)

The complete flow diagram of the GA Algorithm is shown in Figure 5. In general, there are three stages to the search process in GA: Phase one involves creating an initial population, Phase two involves evaluating a fitness function, and Phase three involves creating a new population. The fitness function is the only variable that the genetic algorithm (GA) optimizes. As a result, the problem's objective function and some of its constraints must be translated into a fitness metric. The fitness function measures the quality of chromosomes, and it is closely related to the objective function. The values of different parameters used during the optimization process are depicted in Appendix A.12. The initial population is generated randomly, with individuals within the bounds set

for each independent variable of the problem. A statistical parameter comparison was done for both algorithms for PV placement.

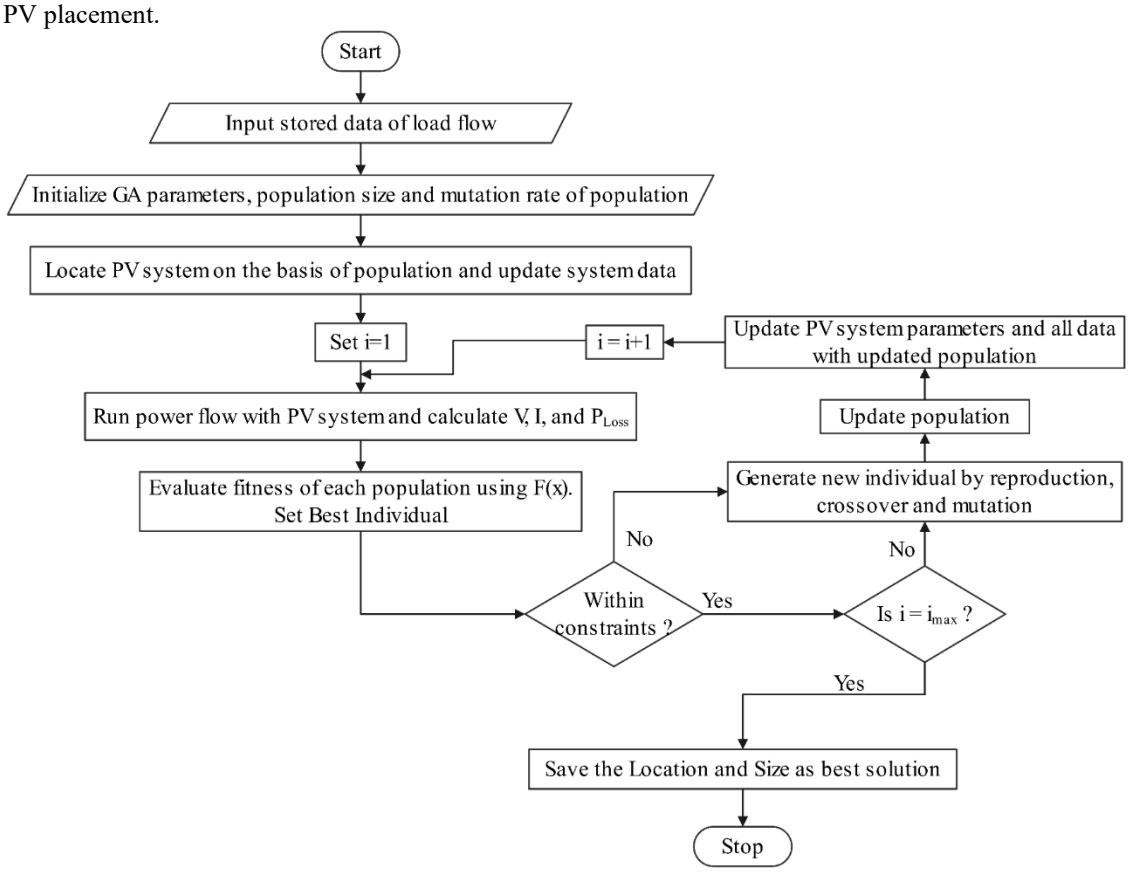

Figure 5 Flowchart for Optimal Placement and Size of PV system using GA

3.3. Technical and Economic Analysis

A statistical parameter comparison is performed for both algorithms, focusing on PV sizing and location, over 200 iterations. After determining the optimal size and location for single- and multi-PV systems, an economic analysis was conducted between them. The investment cost for installing PV systems, and the loss cost they reduced by decreasing power loss in the system, were calculated, and their ratio was determined. The load factor (LF) was calculated by taking the average load and maximum load for a particular day, and the loss of load factor (LLF) was calculated to calculate the annual total power loss cost as shown in equations (16) and (17), respectively.

$$\text{Load Factor (LF)} = \frac{\text{Average load}}{\text{maximum load}} \tag{15}$$

$$\text{Load Loss Factor (LLF)} = (0.2 * \text{LF}) + (0.8 * \text{LF2}) \tag{16}$$

$$\text{Annual total power loss cost} = \text{LLF} * \text{Active power loss} * \text{Per unit energy cost} * 8760 \tag{17}$$

The system with the lowest investment-to-cost-saving ratio was selected as best suited from the economic analysis.

3.4. Voltage Stability Analysis

As the active power flow increases, the receiving end voltage of the line decreases. Low voltages at the receiving end will lead to elevated active and reactive power losses across the line [47]. The system's steady-state voltage stability is observed under two scenarios: integrating the PV only and combining PV with the capacitor bank.

P-V curves illustrate the relationship between the load demand in MW in a specific area and the corresponding bus voltage for different power factors. The relation between P and V is non-linear, it involves the

full power flow solution [48]. In this work, the slack bus serves as the source, while all the loads are considered sinks. The real power transfer increases at a constant power factor, and the bus voltages are monitored.

After conducting a sensitivity analysis, the most sensitive buses in the system were identified, and the P-V curve was plotted for these buses. A comparison of the base case and the case after integrating PVs was conducted to assess the changes in loading margin, critical voltage, critical point, and collapse margin of the system. Carrying the sensitivity analysis dV/dP and dV/dQ, the most critical buses of the network are identified, and steady-state voltage stability for these buses is checked after integration of the best-suited DGs from the economic analysis. P-V curve is plotted to look after the collapse margin and critical voltages for most critical buses.

4. Result and Analysis

4.1. System Description

4.2. IEEE 33-bus Radial Distribution System

The IEEE 33 bus radial distribution system has been used as a candidate test bus in this research. The load flow analysis for the base case, as well as after PV integration, was carried out for this system using MATLAB. The single-line diagram of the IEEE 33-bus Radial Distribution System is shown in Figure 6 [49].

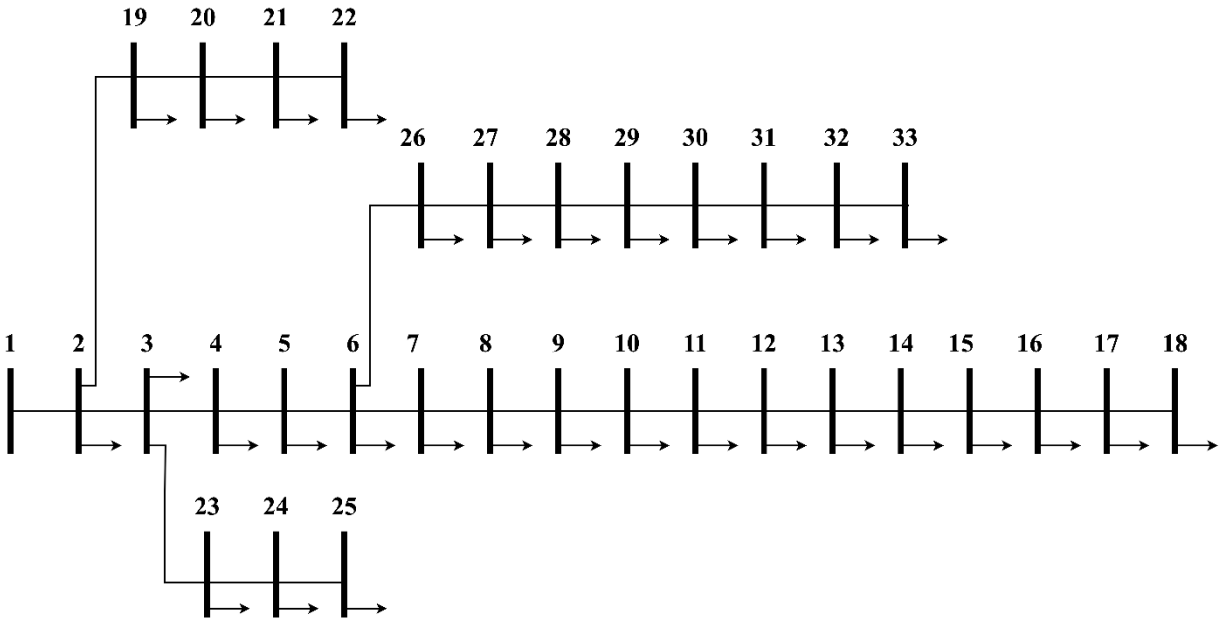

Figure 6 Single line diagram of IEEE 33 test bus system

4.2.1. Panbari Feeder

The Panbari feeder is one of the longest feeders of the Dharan substation, located in Hariyali, Dharan District, Nepal. Being an outdoor substation, the switchyard is supplied with a 33 kV incomer from the Duhabi substation. Among the seven distinct feeders of the Dharan substation, the Panbari feeder has more scattered loads, such as Purwanchal Campus, Radio Nepal, and Purano Crusher, with a gross feeder length of 26.3 km. For 11 kV lines, a Rabbit conductor is used. Altogether, the feeder comprises 48 transformers. While modeling the network, the feeder is lumped into 40 40-bus system with transformers located within a 100-meter radius, with a single bus with a load as depicted in Figure 7. Static loads are considered to have a power factor of 0.8 lagging. The sum of individual loads is taken as the total transformer load.

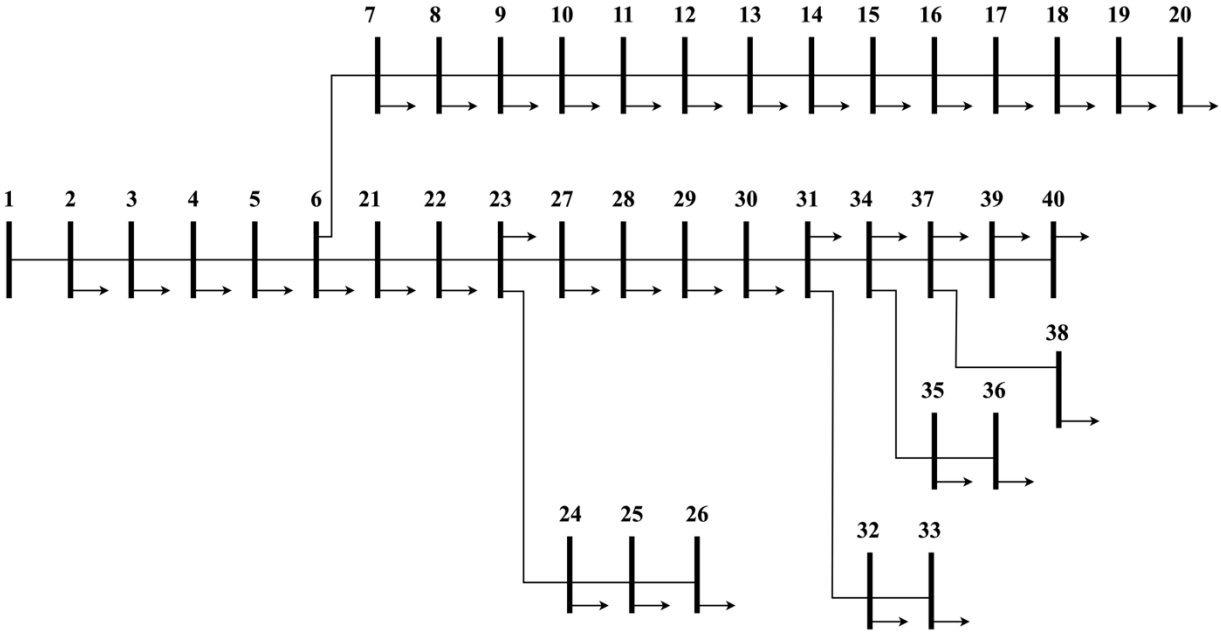

Figure 7 Single line diagram of modified Panbari feeder 40 bus RDS

4.3. Analysis of IEEE 33 bus Radial Distribution System

4.3.1. Optimization with PSO

For the optimal sizing and siting of single- and multi-PV systems, PSO is used to minimize active power loss as the objective function. For single PV, 48.95% loss reduction is achieved when PV of size 2664 kW is penetrated at bus 11. Similarly, a loss reduction of 69.55% was achieved with the integration of DG (PV with capacitor bank) of size 2924 kVA in bus 6. In both cases for single DG penetration, the voltage profile was within the limit. The minimum voltage at bus 18, 0.913 pu, was improved to 0.953 pu, which is an acceptable voltage limit of 5% margin in the distribution system voltage level. All the voltages are in the permissible limit of 1± 0.05 pu. With two PVs of 883 kW at bus 13 and 1,180 kW at bus 30, the loss has been reduced by 58.56%, bringing the voltage profile within the limits. Similarly, an 85.81% loss reduction is observed with the integration of two distributed generators (DGs) of sizes 1071 kVA and 1508 kVA at buses 12 and 30, respectively. With the integration of three PV systems of sizes 780 kW, 1075 kW, and 1120 kW at buses 14, 24, and 30, respectively, the loss has been reduced by 65.54%. Similarly, with the integration of three DGs of sizes 830 kVA, 1199 kVA, and 1488 kVA at buses 14, 24, and 30 respectively, the loss has been reduced by 94.23%.

4.3.2. Optimization with GA

For the optimal sizing and siting of single- and multi-PV systems, GA is used to minimize active power loss as the objective function. With the penetration of 2664 kW PV at bus 11, a 48.95% loss reduction was observed using GA, a similar case to that of PSO. Similarly, a 69.17% loss reduction was observed with the integration of a 3131 kVA size DG (PV with capacitor bank) in bus 6 using GA. In both cases for single DG penetration, the voltage profile remains within the limit, with a voltage of 0.953 pu at bus number 18. Two PV systems of sizes 873 kW at bus 12 and 1,212 kW at bus 30 have been observed to reduce the loss by 58.83%, thereby improving the voltage profile. Similarly, 85.56% loss reduction is seen with the integration of two DGs of size 933 kVA and 1564 kVA at buses 13 and 30 respectively. All the voltages are within the permissible limit after the two DG integrations. The loss reduction of 62.53% has been seen integrating three PV of sizes 1162 kW, 638 kW, and 747 kW at buses 6, 14, and 31 respectively having voltage profiles within the limit range with a minimum voltage of 0.977 pu at bus 33. Similarly, a loss reduction of 93.50% has been achieved by integrating three DGs of sizes 1045 kVA, 1167 kVA, and 1363 kVA at buses 11, 24, and 30 respectively with minimum voltage being 0.9866 pu at bus 18.

The convergence plot for both the algorithms with objective functions respective to iterations is shown in Figure 8. For both cases, the function has converged within the specified number of iterations.

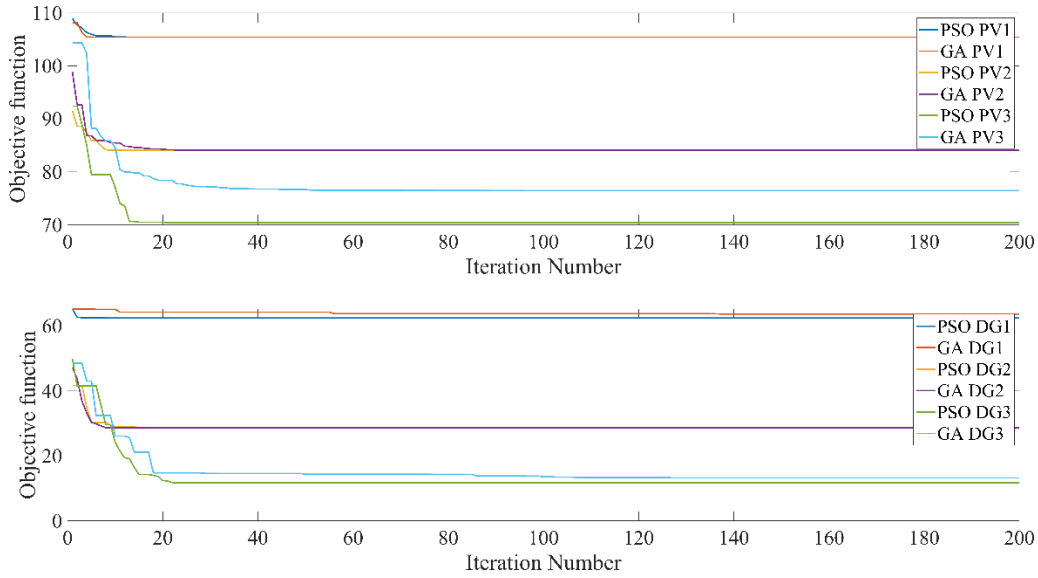

Figure 8 Convergence plot for multi-scenario DG placement in the IEEE 33 test bus system

Figure 9 and Figure 10 show the voltage profile after the integration of PV only and PV with the capacitor bank and Figure 11 shows the scenario of power loss with DGs integration for the best objective function fit scenario among PSO and GA for IEEE 33 test bus system.

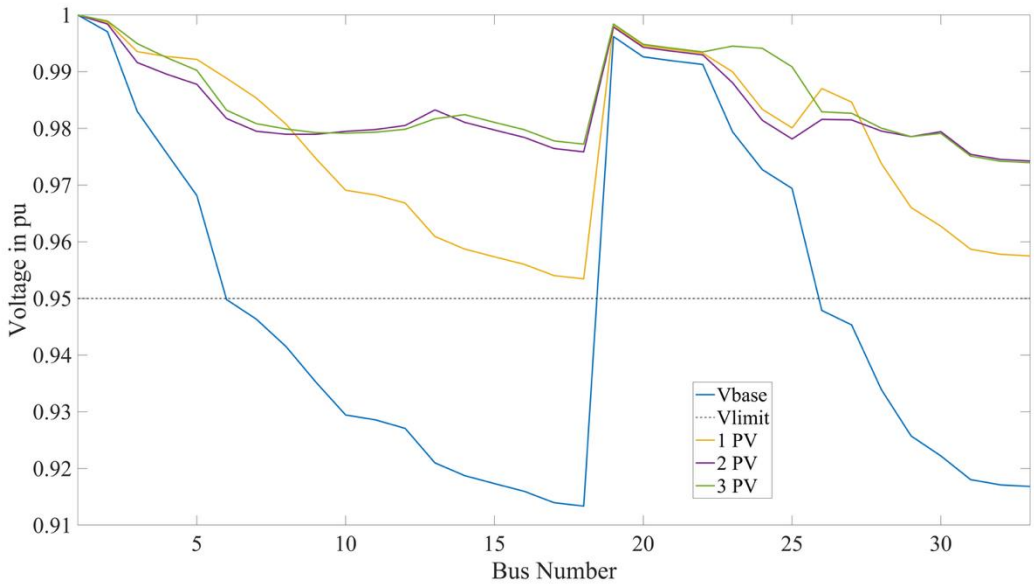

Figure 9 Voltage profile with the integration of PVs in IEEE 33 test bus system

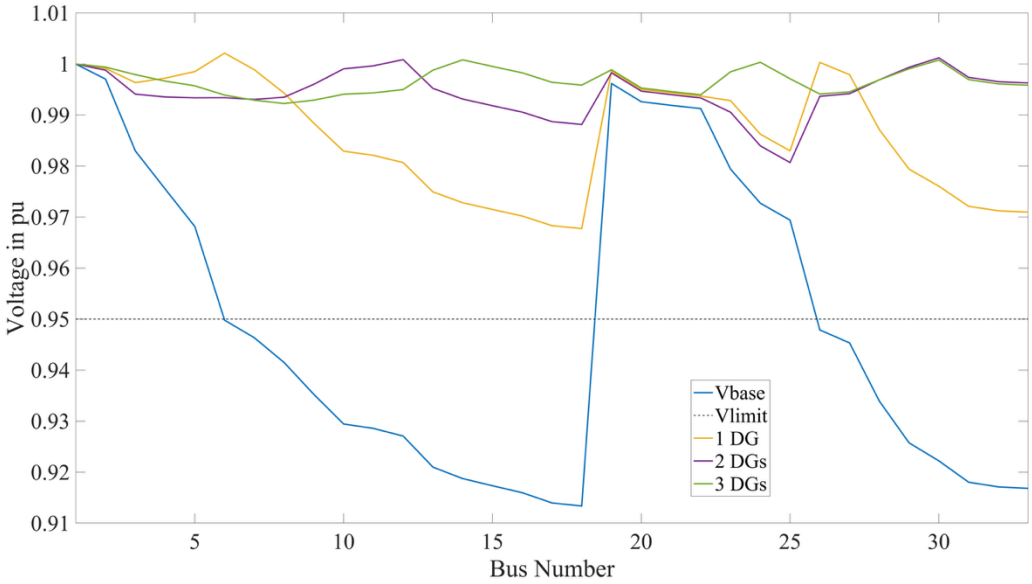

Figure 10 Voltage profile with the integration of PVs and capacitor banks in IEEE 33 test bus system

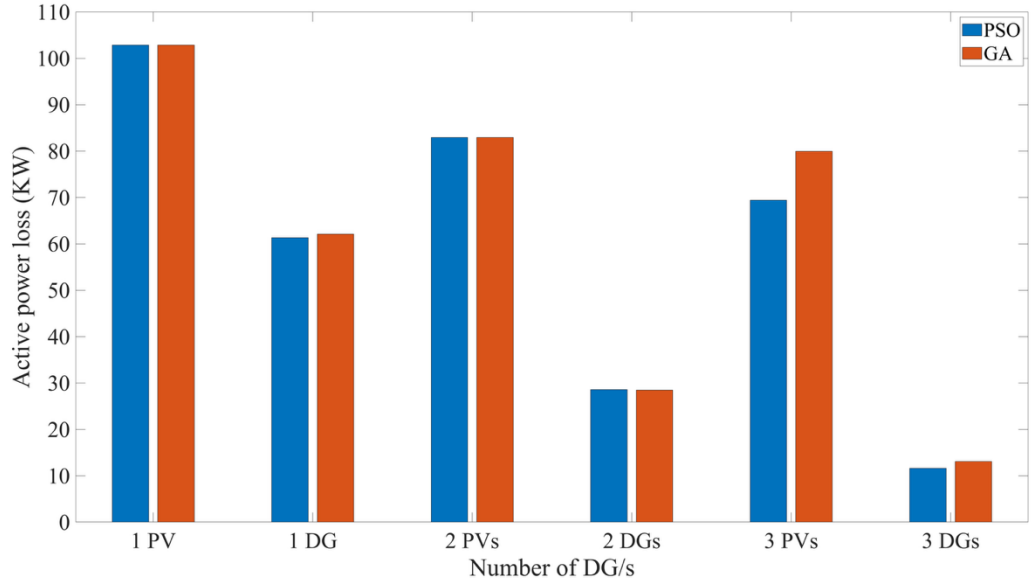

Figure 11 Power loss scenarios with DGs integration in IEEE 33 test bus system

Table 1 and Table 2 show the optimized sizing and location for multi-scenario DG placement with a percentage reduction in active power loss for all cases using PSO and GA in the IEEE 33 test bus system.

Table 1 Loss reduction scenario with PV, IEEE 33 test bus system

Algorithm	L1	S1 (KW)	L2	S2 (KW)	L3	S3 (KW)	Active power loss (KW)	% loss reduction
Base	-	-	-	-	-	-	201.49	-
PSO	11	2664	-	-	-	-	102.87	48.95
	13	883	30	1180	-	-	83.50	58.56
	14	780	24	1075	30	1120	69.43	65.54
GA	11	2664	-	-	-	-	102.87	48.95
	12	873	30	1212	-	-	82.95	58.83
	6	1162	14	638	31	747	75.50	62.53

Table 2 Loss reduction scenario with PV and capacitor bank, IEEE 33 test bus system

Algorithm	L1	S1		L2	S2		L3	S3		Active power loss (KW)	%loss reduction
		KW	KVAR		KW	KVAR		KW	KVAR		
Base	-	-	-	-	-	-	-	-	-	201.49	-
PSO	6	2510	1500	-	-	-	-	-	-	61.35	69.55
	12	969	456	30	1093	1039	-	-	-	28.59	85.81
	14	752	351	24	1080	521	30	1053	1051	11.63	94.23
GA	6	2583	1770	-	-	-	-	-	-	62.11	69.17
	13	845	396	30	1146	1065	-	-	-	28.49	85.86
	11	967	397	24	1012	581	30	1003	923	13.09	93.50

Table 3 Result comparison of IEEE 33 test bus system

Algorithm	Reference	DG sizes (KW)	DG locations	Reduction of power loss %	Minimum voltage pu
PSO	work	780, 1075, 1120	14, 24, 30	65.54	0.974
GA		1162, 638, 747	6, 14, 31	62.53	0.977
CLPSO	[37]	930, 850, 1050	11, 32, 24	65.64	0.981
PSO- Analytical	[38]	790, 1070, 1010	13, 24, 30	65.45	0.970
HPSO	[39]	560, 560, 790	8, 13, 31	60.26	0.966
GA-PSO	[49]	925, 863, 1200	11, 16, 32	49.2	0.967

4.4. Analysis of Panbari Feeder

4.4.1. Optimization with PSO

For the optimal sizing and siting of single and multi-PV systems, PSO is used to minimize active power loss as an objective function. For single PV, 63.06% loss reduction is achieved when a PV of size 3996 kW is penetrated at bus 27. Similarly, a loss reduction of 85.60% was achieved with the integration of DG (PV with capacitor bank) of size 4121 kVA in bus 28. In both cases for single DG penetration, the voltage profile is not within the limit being 0.928 pu voltage at bus number 20. With two PVs of size 1096 kW at bus 13 and 2795 kW at bus 30, the loss has been reduced by 63.06% bringing the voltage profile within the limits. Similarly, 94.05% loss reduction is seen with the integration of two DGs of size 2263 kVA and 2532 kVA at buses 9 and 31 respectively. With the integration of three PV of sizes 1785 kW, 750 kW, and 1831kW at buses 6, 15, and 34 respectively, the loss has been reduced by 71.03% and the voltage profile has significantly improved with minimum voltage being 0.972 pu at bus number 26. Similarly, with the integration of three DGs of sizes 1030 kVA, 2238 kVA, and 1593 kVA at buses 13, 23, and 37 respectively, the loss has been reduced by 97.82%.

4.4.2. Optimization with GA

For optimal sizing and siting of single and multi-PV systems, GA is used for minimizing the active power loss as an objective function. With the penetration of 4009 kW PV at bus 27, 63.07% loss reduction was seen

using GA. Similarly, 84.64% loss reduction was seen with the integration of 4041 kVA size DG (PV with capacitor bank) in bus 28 using GA. In both cases for single DG penetration, the voltage profile is not within the limit being 0.929 pu voltage at bus numbers 18, 19, and 20. Two PV of size 1114 kW at bus 13 and 2745 kW at bus 30 have to reduce the loss by 63.07% improving the voltage profile. Similarly, 94.0% loss reduction is seen with the integration of two DGs of size 2341 kVA and 2472 kVA at buses 9 and 31 respectively. All the voltages are within the permissible limit after the two DG integrations. The loss reduction of 71.09% has been seen integrating three PV of sizes 886 kW, 1460 kW, and 1829 kW at buses 14, 23, and 37 respectively with voltage profile at limit range having a minimum voltage of 0.974 pu at bus 19 and 20. Similarly, a loss reduction of 97.98% has been achieved by integrating three DGs of sizes 2290 kVA, 813 kVA, and 2012 kVA at buses 6, 15, and 34 respectively with minimum voltage being 0.995 pu from buses 24 to 28.

The results in terms of voltage profile improvement and reduction in power loss of the system are computed after the placement of DGs for both systems.

The convergence plot for both the algorithms with objective function, respective to iterations, is shown in Figure 12. For both the cases, the function has been converged within tried iterations.

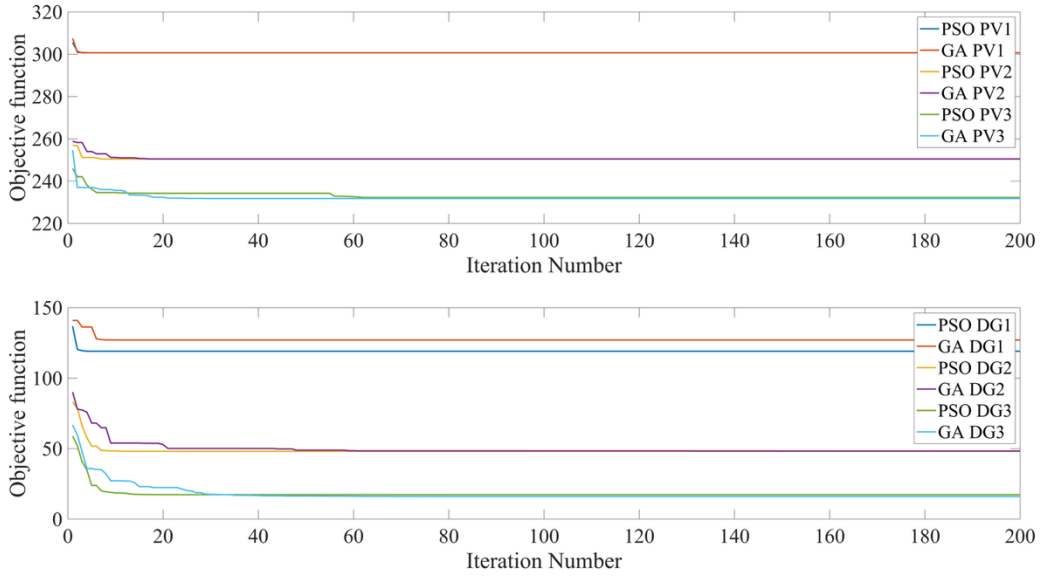

Figure 12 Convergence plot for multi-scenario DG placement in Panbari feeder

Figure 13 and Figure 14 shows the voltage profile after integration of PV only and PV with capacitor bank and Figure 15 shows the scenario of power loss with DGs integration for best the objective function fit scenario among PSO and GA for Panbari Feeder.

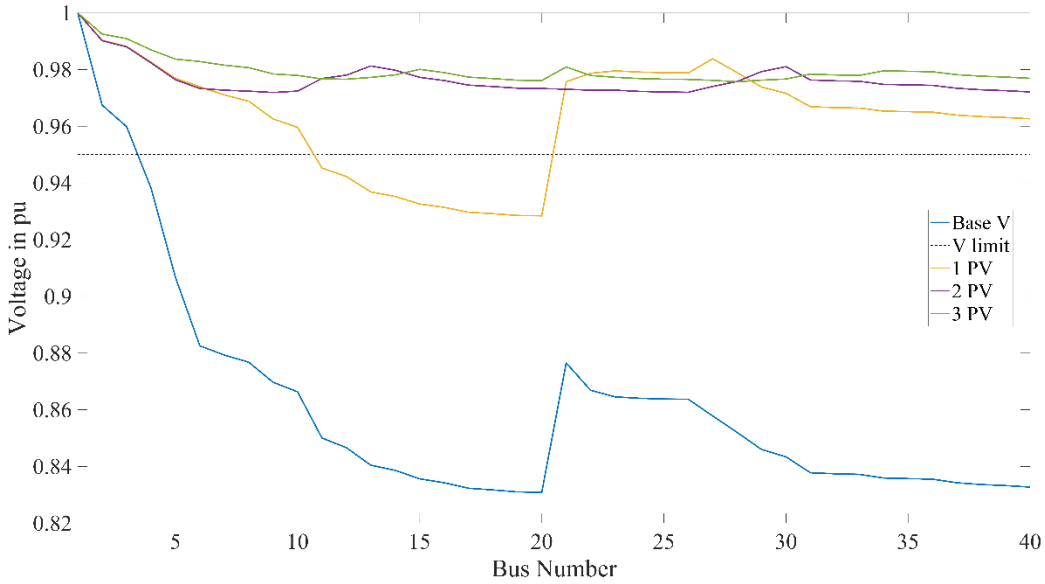

Figure 13 Voltage profile with integration of PVs in Panbari feeder

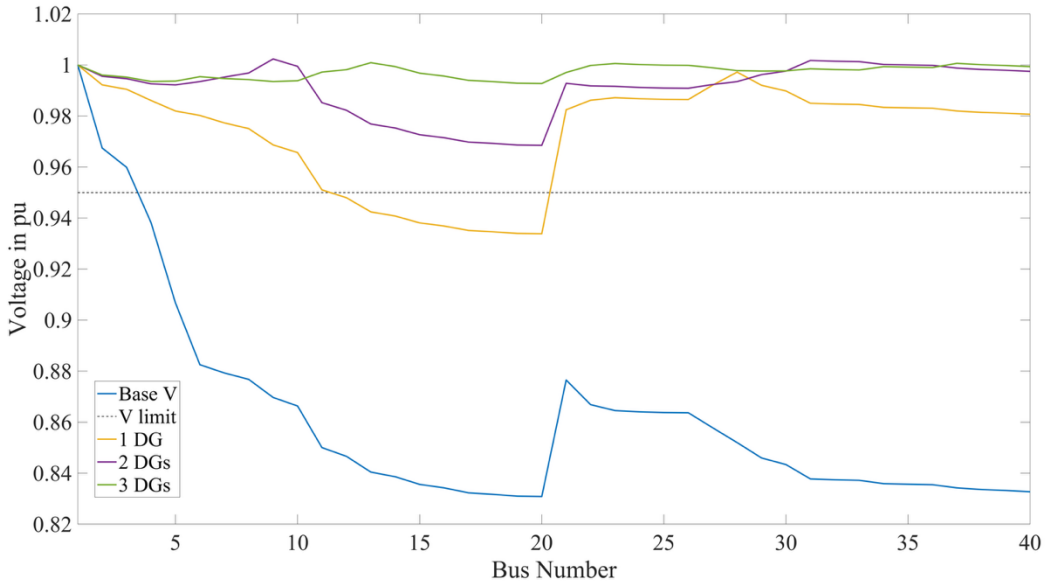

Figure 14 Voltage profile with integration of DGs in Panbari feeder

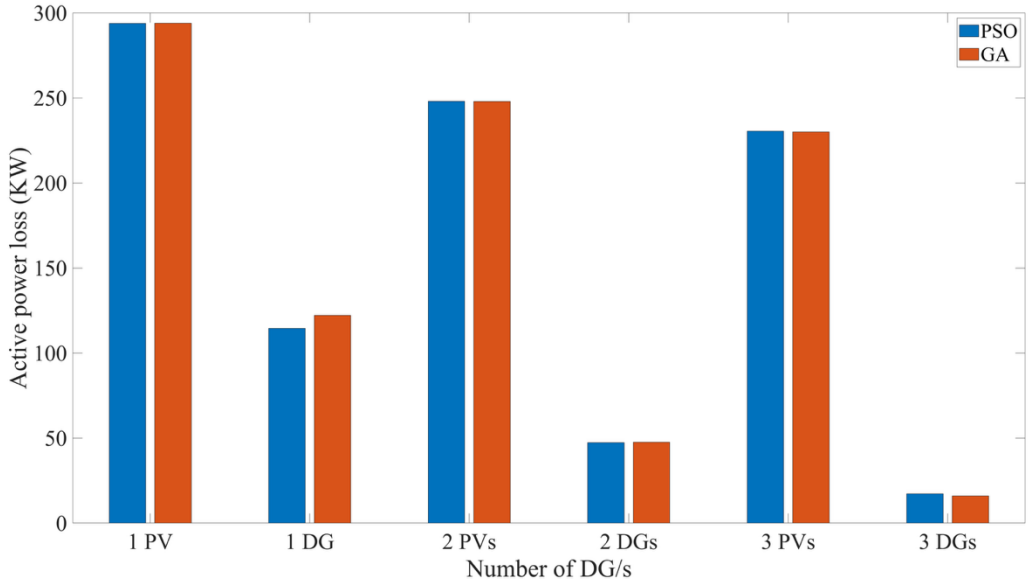

Figure 15 Power loss scenarios with DGs integration in Panbari feeder

Table 4 and Table 5 shows the optimized sizing and location for multi-scenario DG placement, along with the percentage reduction in active power loss for all cases using PSO and GA in the Panbari feeder.

Table 4 Loss reduction scenario with PV, Panbari feeder

Algorithm	L1	S1 (KW)	L2	S2 (KW)	L3	S3 (KW)	Active power loss (KW)	% loss reduction
Base	-	-	-	-	-	-	795.75	-
PSO	27	3996	-	-	-	-	293.97	63.06
	30	2795	13	1096	-	-	248.09	68.82
	6	1785	34	1831	15	750	230.54	71.03
GA	27	4009	-	-	-	-	293.89	63.07
	30	2745	13	1114	-	-	248.01	68.83
	23	1829	37	1460	14	886	230.05	71.09

Table 5 Loss reduction scenario with PV and capacitor bank, Panbari feeder

Algorithm	L1	S1		L2	S2		L3	S3		Active power loss (KW)	%loss reduction
		KW	KVAR		KW	KVAR		KW	KVAR		
Base	-	-	-	-	-	-	-	-	-	795.75	-
PSO	28	3598	2010	-	-	-	-	-	-	114.55	85.60
	31	2040	1500	9	1805	1366	-	-	-	47.36	94.05
	23	1791	1342	37	1275	956	13	825	617	17.33	97.82
GA	28	3613	1811	-	-	-	-	-	-	122.20	84.64
	31	1995	1460	9	1883	1391	-	-	-	47.61	94.02
	6	1832	1373	34	1610	1207	15	651	488	16.04	97.98

4.5. Statistical Parameters Comparison

Table 6 shows the statistical parameter comparison between the two algorithms used, PSO and GA for the placement of PV and PV with a capacitor bank in the modified Panbari 40 bus system respectively. In both cases, the standard deviation is larger for the PSO algorithm than GA, whereas the computational time for GA is more than that of GA.

Table 6 Statistical parameters comparison for PSO and GA

	PV Only		**PV and Capacitor**	
	PSO	GA	PSO	GA
Minimum value (KW)	232.31	231.83	17.38	16.07
Maximum value (KW)	312.75	319.79	173.33	196.80
Mean value (KW)	272.53	275.81	95.36	106.44
Standard deviation	0.21	0.20	1.48	0.80
Computational time (seconds)	62	84	88	114

4.6. Economic Analysis

Economic analysis among single and multi-DG case scenarios is done to select the most suitable number of DGs. The cost of solar PV installment is taken as 60 million NRP (excluding land cost factor) for 1000 kW size [50], the cost of the capacitor bank is taken 1920 NRP for 1 kVAR [51] and the tariff rate of electricity is taken average NRP Rs. 11/kWh. For calculating the annual loss cost, load factor and loss load factor are calculated. The economic analysis for PV integration in Parbari feeder is as shown in Table 7 and Table 8 shows the economic analysis for both PV and Capacitor bank placement in multi-scenarios.

Table 7 Economic analysis for PV integration in Panbari feeder

Base Case	Loss (KW)	795.75
	Loss of energy per annum (KWh)	6970770
	Loss cost (Million NRP)	52.91
1 PV	Loss (KW)	293
	Loss of energy per annum (KWh)	2566680
	Loss cost (Million NRP)	19.48
	Saving Cost (Million NRP)	33.43
2 PV	Loss (KW)	248
	Loss of energy per annum (KWh)	2172480
	Loss cost (Million NRP)	16.49
	Saving Cost (Million NRP)	36.42
3 PV	Loss (KW)	230
	Loss of energy per annum (KWh)	2014800
	Loss cost (Million NRP)	15.29
	Saving Cost (Million NRP)	37.62

Table 8 Economic analysis for PV and capacitor bank integration in Panbari feeder

Base Case	Loss (KW)	795.75
	Loss of energy per annum (KWh)	6970770.00
	Loss cost (Million NRP)	52.91
1 DG	Loss (KW)	114.00
	Loss of energy per annum (KWh)	998640.00
	Loss cost (Million NRP)	7.58
	Saving Cost (Million NRP)	45.33
2 DG	Loss (KW)	47.00
	Loss of energy per annum (KWh)	411720.00
	Loss cost (Million NRP)	3.12
	Saving Cost (Million NRP)	49.78
3 DG	Loss (KW)	16.00
	Loss of energy per annum (KWh)	140160.00
	Loss cost (Million NRP)	1.06
	Saving Cost (Million NRP)	51.84

Table 9 shows the investment saving ratio for multi-scenario DG placement, among which 2 DG is selected as best best-suited option among the three scenarios with the lowest investment saving ratio. The investment-to-saving ratio for the integration of two DG systems is minimum, so it is best suited from economic analysis.

Table 9 Investment saving ratio for DG placement

Number of DG	PV Size (KW)	Capacitor size (KVAR)	Investment Cost (Million NRP)	Investment Saving Ratio
1	3598	2010	219.7392	4.85
2	2040, 1805	1500, 1366	238.18272	4.78
3	1832, 1610,651	1373, 1207,488	251.47056	4.85

4.7. Sensitivity Analysis

Load flow sensitivity analysis is carried out to investigate the most sensitive bus in the distribution system. From dV/dP and dV/dQ sensitivity analysis, buses 18, 19, and 20 are found to be the most sensitive buses in the network respectively. Since no value of dV/dP and dV/dQ is negative for base and for DG integration scenario, the system voltage is in stable region [52]. The PV curve for these three buses is plotted to check for steady-state voltage analysis before and after the integration of two DGs, which is best selected from the economic analysis.

The observations from the P-V curves are shown in Table 10. The collapse margin has shifted to 2.194 MW with integration of two PV at bus 13 and 30. Also, with integration of two PV with capacitor bank at bus 9 and 31, the collapse margin has shifted to 2.045 MW. The critical voltage for most sensitive buses has shifted gradually with DG integration enhancing voltage stability in the distribution system. Figure 16, Figure 17, and Figure 18 show the P-V curves for the three most sensitive buses: 18, 19 and 20.

Table 10 Observation from the PV curve for the three most sensitive buses

Parameters		**Base case**	**with 2 PV**	**with 2 PV and Capacitor bank**
Collapse margin (Pm) (MW)		1.522	2.194	2.045
Critical voltage (pu)	Bus 18	0.453	0.506	0.516
	Bus 19	0.439	0.487	0.499
	Bus 20	0.436	0.483	0.495

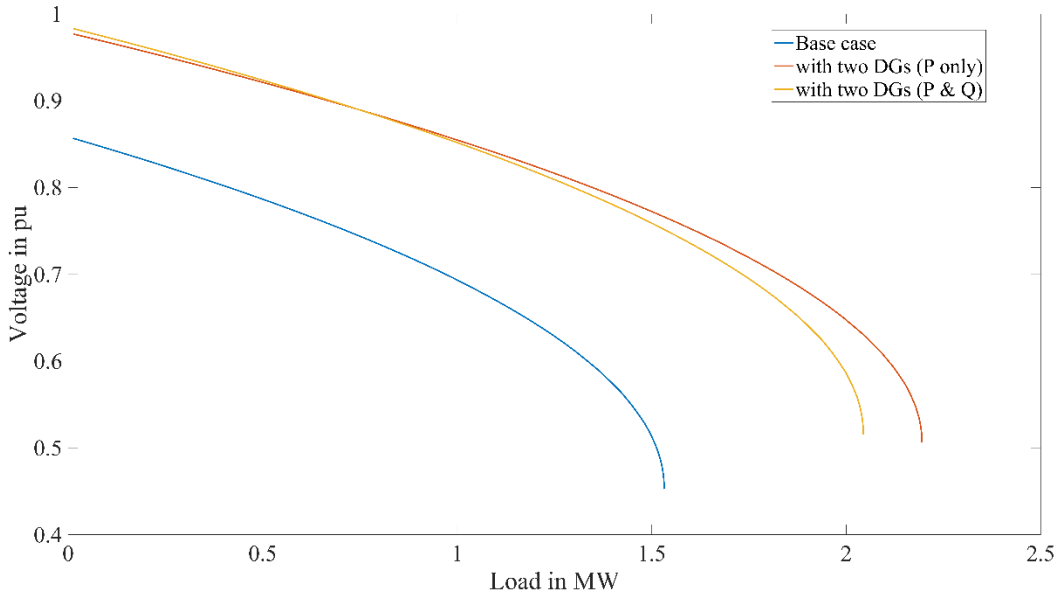

Figure 16 P-V curve for Bus 18, Panbari feeder

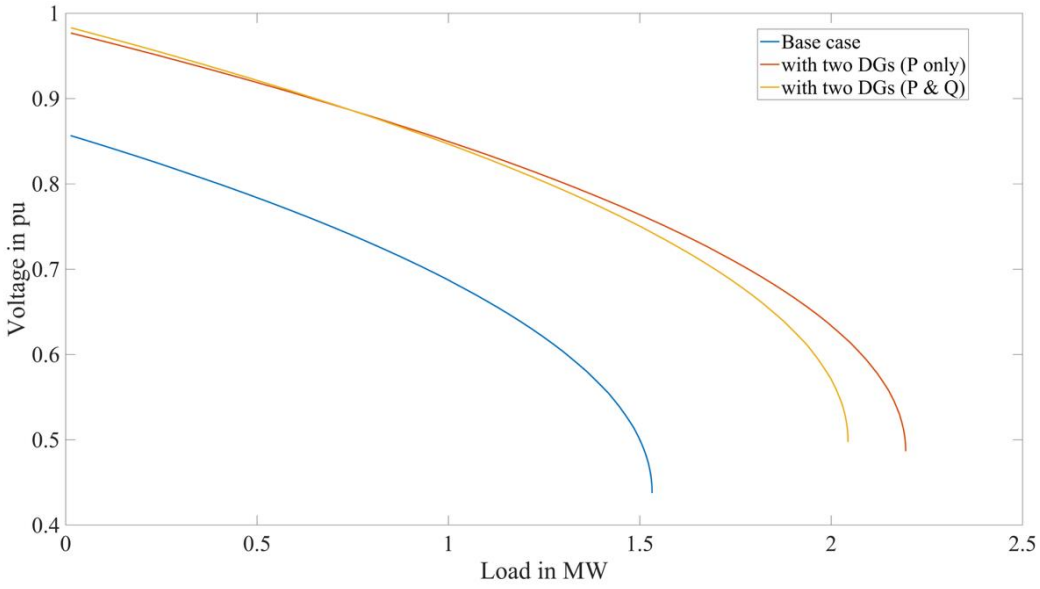

Figure 17 P-V curve for Bus 19, Panbari feeder

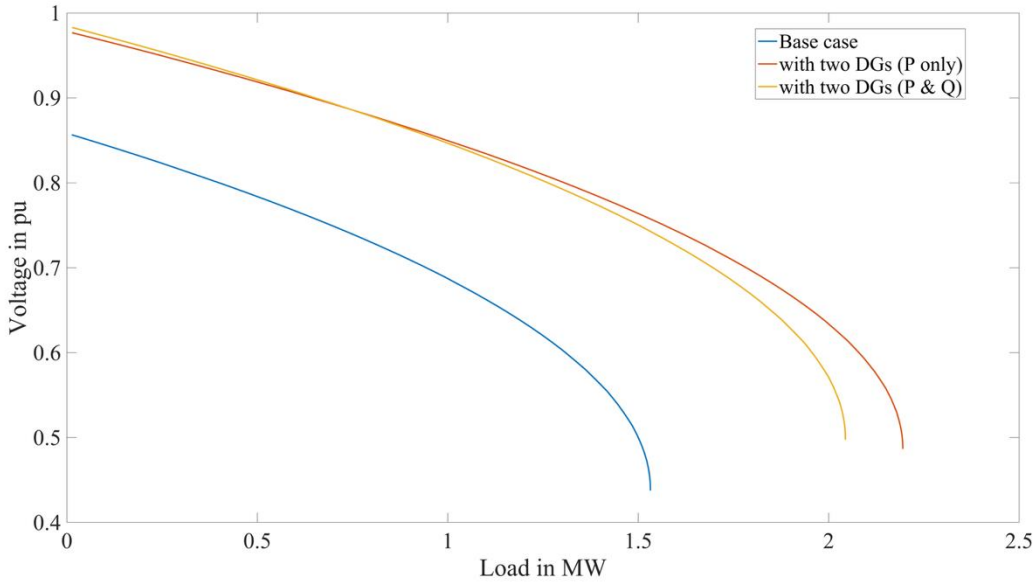

Figure 18 P-V curve for Bus 20, Panbari feeder

5. Conclusion

Simulation results show that the integration of solar photovoltaic and other forms of distributed generation in radial distribution systems results in an improvement of the voltage profile and a substantial reduction in power losses. By applying PSO and GA, the optimal placement and sizing of single and multi-PV units were determined. PSO was seen as faster in terms of computation and convergence speed than GA for the same number of populations. From economic analysis, the integration of two PV systems was found to be best for the Panbari feeder. Additionally, after DG integration, the steady-state voltage stability of the most sensitive buses improved, accompanied by an increase in the loading margin of the bus.

The various conclusions that can be drawn from these works are mentioned below:

a. Integration of PV only or PV with capacitor banks in a radial distribution system result in improvement of the voltage profile and a decrease in line losses of the system. PV with a capacitor bank has shown better voltage profile improvement with more reduction in line losses than PV only integration.
b. Among single and multi-PV, integration of two PV is found to be the best from economic analysis.
c. Improvement in steady-state voltage stability is observed for the most sensitive buses after PV integration, with an increase in loading margin and a shifted critical voltage point.

The work mainly emphasizes the impact analysis for DG integration in the distribution system, while fewer assumptions are made during system modelling, such as the consideration of static load and lumping of nearby buses into a single bus. Similarly, the land cost factor is not considered for the economic analysis. Further work can incorporate these limitations, considering dynamic load models and a probabilistic approach to integrate photovoltaic generation into the grid.

Appendix A. Parameters used in optimization

Table A.11: Particle Swarm Optimization

Parameter	Value
Population size	150
Number of iterations	200
Inertia weight (ω)	1.0
Inertia weight damping ratio (ωdamp)	1.5
Personal learning coefficient (c1)	1.5
Global learning coefficient (c2)	2.0

Table A.12: Genetic Algorithm

Parameter	Value
Population size	150
Number of iterations	200
Linear crossover	0.85
Crossover probability	0.9
Mutation probability	0.1
Mutation rate	0.2

Conflict of Interest

There is no conflict of interest for this study.

References

[1] E. Kabir, P. Kumar, S. Kumar, A. A. Adelodun, and K.-H. Kim, "Solar energy: Potential and prospects," Renewable and Sustainable Energy Reviews, vol. 82, pp. 894–900, 2018.

[2] R. Panigrahi, S. K. Mishra, S. C. Srivastava, A. K. Srivastava, and N. N. Schulz, "Grid integration of small-scale photovoltaic systems in secondary distribution network—A review," IEEE Trans Ind Appl, vol. 56, no. 3, pp. 3178–3195, 2020.

[3] A. S. N. Huda and R. Živanović, "Large-scale integration of distributed generation into distribution networks: Study objectives, review of models and computational tools," Renewable and Sustainable Energy Reviews, vol. 76, pp. 974–988, 2017.

[4] T. Ackermann, G. Andersson, and L. Söder, "Distributed generation: a definition," Electric Power Systems Research, vol. 57, no. 3, pp. 195–204, 2001.

[5] S. Howell, Y. Rezgui, J.-L. Hippolyte, B. Jayan, and H. Li, "Towards the next generation of smart grids: Semantic and holonic multi-agent management of distributed energy resources," Renewable and Sustainable Energy Reviews, vol. 77, pp. 193–214, 2017.

[6] R. Gautam, S. Khadka, T. B. Malla, A. Bhattarai, A. Shrestha, and F. Gonzalez-Longatt, "Assessing uncertainty in the optimal placement of distributed generators in radial distribution feeders," Electric Power Systems Research, vol. 230, p. 110249, 2024.

[7] M. S. Mahmoud and M. Fouad, "Control and optimization of distributed generation systems," 2015.

[8] U. Sultana, A. B. Khairuddin, M. M. Aman, A. S. Mokhtar, and N. Zareen, "A review of optimum DG placement based on minimization of power losses and voltage stability enhancement of distribution system," Renewable and Sustainable Energy Reviews, vol. 63, pp. 363–378, 2016.

[9] S. Bruno, S. Lamonaca, G. Rotondo, U. Stecchi, and M. La Scala, "Unbalanced three-phase optimal power flow for smart grids," IEEE Transactions on Industrial Electronics, vol. 58, no. 10, pp. 4504–4513, 2011.

[10] R. O. Bawazir and N. S. Cetin, "Comprehensive overview of optimizing PV-DG allocation in power system and solar energy resource potential assessments," Energy Reports, vol. 6, pp. 173–208, 2020.

[11] S. Abbas, K. Techato, L.-H. C. Hsieh, and A. M. Sadeq, "Integrating relational values in social acceptance of photovoltaic energy storage systems: A consumers' perspective assessment using structural equation modeling," Energy, vol. 304, p. 132092, 2024.

[12] M. Bošnjaković, R. Santa, Z. Crnac, and T. Bošnjaković, "Environmental impact of PV power systems," Sustainability, vol. 15, no. 15, p. 11888, 2023.

[13] E. H. Sepulveda-Oviedo, "Impact of environmental factors on photovoltaic system performance degradation," Energy Strategy Reviews, vol. 59, p. 101682, 2025.

[14] M. Karimi, H. Mokhlis, K. Naidu, S. Uddin, and A. H. A. Bakar, "Photovoltaic penetration issues and impacts in distribution network–A review," Renewable and Sustainable Energy Reviews, vol. 53, pp. 594–605, 2016.

[15] E. Liu and J. Bebic, "Distribution system voltage performance analysis for high-penetration photovoltaics," 2008.

[16] K. Jadeja, "Major technical issues with increased PV penetration on the existing electrical grid," Murdoch University, 2012.

[17] A. O. Muhammed and M. Rawa, "A Systematic PVQV-Curves approach for investigating the impact of solar photovoltaic-generator in power system using powerworld simulator," Energies (Basel), vol. 13, no. 10, p. 2662, 2020.

[18] P. Lazzeroni, S. Olivero, F. Stirano, and M. Repetto, "Impact of PV penetration in a distribution grid: A Middle-East study case," in 2015 IEEE 1st International Forum on Research and Technologies for Society and Industry Leveraging a better tomorrow (RTSI), 2015, pp. 353–358.

[19] R. Singh, P. Tripathi, and K. Yatendra, "Impact of solar photovoltaic penetration in distribution network," in 2019 3rd international conference on recent developments in control, automation & power engineering (RDCAPE), 2019, pp. 551–556.

[20] A. I. Nousdilis, A. I. Chrysochos, G. K. Papagiannis, and G. C. Christoforidis, "The impact of Photovoltaic Self-Consumption Rate on voltage levels in LV distribution grids," in 2017 11th IEEE International Conference on Compatibility, Power Electronics and Power Engineering (CPE-POWERENG), 2017, pp. 650–655.

[21] E. Tsiaras, D. N. Papadopoulos, C. N. Antonopoulos, V. G. Papadakis, and F. A. Coutelieris, "Planning and assessment of an off-grid power supply system for small settlements," Renew Energy, vol. 149, pp. 1271–1281, 2020.

[22] F. Itote, G. Irungu, and M. Saulo, "Power quality assessment of renewable energy sources integration on mv networks," Int. J. Sci. Technol. Res, vol. 8, pp. 1972–1979, 2019.

[23] S. B. Mohod, V. R. Parihar, and S. D. Nimkar, "Hybrid power system with integration of wind, battery and solar PV system," in 2017 IEEE International Conference on Power, Control, Signals and Instrumentation Engineering (ICPCSI), 2017, pp. 2332–2337.

[24] X.-M. Lin, N. Kireeva, A. V Timoshin, A. Naderipour, Z. Abdul-Malek, and H. Kamyab, "A multi-criteria framework for designing of stand-alone and grid-connected photovoltaic, wind, battery clean energy system considering reliability and economic assessment," Energy, vol. 224, p. 120154, 2021.

[25] M. Thebault, V. Clivillé, L. Berrah, L. Gaillard, G. Desthieux, and C. Ménézo, "Multi-criteria decision aiding for the integration of photovoltaic systems in the urban environment: the case of the Greater Geneva agglomeration," Territorio, vol. 1, pp. 9–30, 2020.

[26] K. S. Krishna and K. S. Kumar, "A review on hybrid renewable energy systems," Renewable and Sustainable Energy Reviews, vol. 52, pp. 907–916, 2015.

[27] O. M. Babatunde, J. L. Munda, and Y. Hamam, “A comprehensive state-of-the-art survey on hybrid renewable energy system operations and planning,” IEEE access, vol. 8, pp. 75313–75346, 2020.

[28] F. J. Ruiz-Rodriguez, M. Gomez-Gonzalez, and F. Jurado, “Binary particle swarm optimization for optimization of photovoltaic generators in radial distribution systems using probabilistic load flow,” Electric Power Components and Systems, vol. 39, no. 15, pp. 1667–1684, 2011.

[29] M. Abdel-Salam, M. T. El-Mohandes, and L. Mahmoud, “A PSO-based Multi-objective Method for Optimal Weight Factors, Placement and Sizing of Multiple DG Units in a Distribution System,” in 2019 21st International Middle East Power Systems Conference (MEPCON), 2019, pp. 914–920.

[30] D. Asija and P. Choudekar, “Congestion management using multi-objective hybrid DE-PSO optimization with solar-ess based distributed generation in deregulated power Market,” Renewable Energy Focus, vol. 36, pp. 32–42, 2021.

[31] C. D. Rodr\’\iguez-Gallegos et al., “Placement and sizing optimization for PV-battery-diesel hybrid systems,” in 2016 IEEE International Conference on Sustainable Energy Technologies (ICSET), 2016, pp. 83–89.

[32] S. Essallah, A. Bouallegue, and A. Khedher, “Optimal placement of PV-distributed generation units in radial distribution system based on sensitivity approaches,” in 2015 16th International Conference on Sciences and Techniques of Automatic Control and Computer Engineering (STA), 2015, pp. 513–520.

[33] Y. Sawle, S. C. Gupta, and A. K. Bohre, “Optimal sizing of standalone PV/Wind/Biomass hybrid energy system using GA and PSO optimization technique,” Energy Procedia, vol. 117, pp. 690–698, 2017.

[34] D. Pandey and J. S. Bhadoriya, “Optimal placement & sizing of distributed generation (DG) to minimize active power loss using particle swarm optimization (PSO),” international journal of scientific & technology research, vol. 3, no. 17, 2014.

[35] V. Vita, “Development of a decision-making algorithm for the optimum size and placement of distributed generation units in distribution networks,” Energies (Basel), vol. 10, no. 9, p. 1433, 2017.

[36] K. Subbaramaiah, P. Sujatha, and others, “Optimal DG unit placement in distribution networks by multi-objective whale optimization algorithm & its techno-economic analysis,” Electric Power Systems Research, vol. 214, p. 108869, 2023.

[37] E. Karunarathne, J. Pasupuleti, J. Ekanayake, and D. Almeida, “Comprehensive learning particle swarm optimization for sizing and placement of distributed generation for network loss reduction,” Indonesian Journal of Electrical Engineering and Computer Science, vol. 20, no. 1, pp. 16–23, 2020.

[38] S. Kansal, V. Kumar, and B. Tyagi, “Hybrid approach for optimal placement of multiple DGs of multiple types in distribution networks,” International Journal of Electrical Power & Energy Systems, vol. 75, pp. 226–235, 2016.

[39] M. A. Tolba, V. N. Tulsky, and A. A. Z. Diab, “Optimal allocation and sizing of multiple distributed generators in distribution networks using a novel hybrid particle swarm optimization algorithm,” in 2017 IEEE conference of Russian young researchers in electrical and electronic engineering (EIConRus), 2017, pp. 1606–1612.

[40] A. Backhaus, “Analyzing the Application of Different Energy Cell Sizes as an Approach for the Integration of Decentralized Renewable Energy Sources,” University of Freiburg.

[41] J. A. P. Lopes, N. Hatziargyriou, J. Mutale, P. Djapic, and N. Jenkins, “Integrating distributed generation into electric power systems: A review of drivers, challenges and opportunities,” Electric power systems research, vol. 77, no. 9, pp. 1189–1203, 2007.

[42] H. Hu, S. S. Yu, and H. Trinh, “A Review of Uncertainties in Power Systems—Modeling, Impact, and Mitigation,” Designs (Basel), vol. 8, no. 1, p. 10, 2024.

[43] M. A. V. Rad, A. Kasaeian, X. Niu, K. Zhang, and O. Mahian, "Excess electricity problem in off-grid hybrid renewable energy systems: A comprehensive review from challenges to prevalent solutions," Renew Energy, vol. 212, pp. 538–560, 2023.

[44] I. U. Salam, M. Yousif, M. Numan, K. Zeb, and M. Billah, "Optimizing distributed generation placement and sizing in distribution systems: a multi-objective analysis of power losses, reliability, and operational constraints," Energies (Basel), vol. 16, no. 16, p. 5907, 2023.

[45] D. Della Giustina, M. Pau, P. A. Pegoraro, F. Ponci, and S. Sulis, "Electrical distribution system state estimation: measurement issues and challenges," IEEE Instrum Meas Mag, vol. 17, no. 6, pp. 36–42, 2014.

[46] H. Maurya, V. K. Bohra, N. S. Pal, and V. S. Bhadoria, "Effect of inertia weight of PSO on optimal placement of DG," in IOP Conference Series: Materials Science and Engineering, 2019, p. 12011.

[47] H. Mortazavi, H. Mehrjerdi, M. Saad, S. Lefebvre, D. Asber, and L. Lenoir, "A monitoring technique for reversed power flow detection with high PV penetration level," IEEE Trans Smart Grid, vol. 6, no. 5, pp. 2221–2232, 2015.

[48] D. V. M. Chary, M. V Subramanyam, and P. Kishor, "PV Curve Method for Voltage Stability and Power Margin Studies," International Journal of Engineering Science and Computing, vol. 7, no. 5, pp. 11867–11869, 2017.

[49] S. H. Dolatabadi, M. Ghorbanian, P. Siano, and N. D. Hatziargyriou, "An enhanced IEEE 33 bus benchmark test system for distribution system studies," IEEE Transactions on Power Systems, vol. 36, no. 3, pp. 2565–2572, 2020.

[50] S. Dutta, N. R. Karki, and A. Mishra, "Techno-Economic Analysis of Grid Connected Rooftop Solar PV System at Head Office of Nepal Bank Limited," in IOE Graduate Conference, 2022.

[51] M. Silwal and S. R. Shakya, "Optimal Allocation of Capacitor Bank in Radial Distribution System for Loss Minimization and Voltage Profile Improvement," 2020.

[52] N. Hosseinzadeh, A. Aziz, A. Mahmud, A. Gargoom, and M. Rabbani, "Voltage stability of power systems with renewable-energy inverter-based generators: A review," Electronics (Basel), vol. 10, no. 2, p. 115, 2021.